Front. Phys. China, 2009, 4(3): 415–419
DOI 10.1007/s11467-009-0035-5

RESEARCH ARTICLE

Simulations of inelastic electron tunneling spectroscopy of semifluorinated hexadecanethiol junctions

Chuan-kui WANG (王传奎)[1](✉), **Bin ZOU** (邹斌)[2], **Xiu-neng SONG** (宋秀能)[1], **Ying-de LI** (李英德)[3], **Zong-liang LI** (李宗良)[1], **Li-li LIN** (蔺丽丽)[1]

[1] *College of Physics and Electronics, Shandong Normal University, Jinan 250014, China*
[2] *College of Science, Minzu University of China, Beijing 100081, China*
[3] *Department of Physics and Electronic Science, Weifang College, Weifang 261061, China*
E-mail: ckwang@sdnu.edu.cn

Received January 20, 2009; accepted February 25, 2009

The inelastic electron tunneling spectroscopy (IETS) of semifluorinated hexadecanethiol junctions is theoretically studied. The numerical results show that the C–F vibration modes of semifluorinated alkanethiol series can not be detected, and the C–H stretching mode in IETS is related to the CH_2 vibration. It is demonstrated that the Raman modes are preferred over IR modes in IETS, which is in good agreement with the experimental measurements presented by Beebe *et al.* [Nano Lett., 2007, 7(5): 1364].

Keywords inelastic electron tunneling spectroscopy, semifluorinated hexadecanethiol, molecular electronics

PACS numbers 75.63.-b, 85.65.+h, 73.63.Rt, 31.15.Ar

1 Introduction

In the last decade, inelastic electron tunneling spectroscopy (IETS) has attracted considerable attention on studying properties of organic molecules. For molecular junctions, as tunneling electrons strongly couple with vibrational modes of molecules, well-resolved peaks can be observed in IET spectra. It is realized that the IETS is an important tool for characterizing the molecular junctions [1−3]. Recently, a variety of experimental and theoretical works on a few kinds of molecules have been carried out for pursuing fundamental rules during the scattering process. Concerning the IETS of molecular junctions, a number of issues such as the temperature dependence [4−6], the molecule–metal contact structure effect [7], the molecular orientation effect [8, 9], the hydration effect [10], and the propensity rules based on the molecular symmetry and on the topology of the molecule in the junction [11−13] have been investigated. A series of propensity rules for interpreting IETS of molecular junctions have thus been revealed. However, these insights are just obtained from a few molecules, and some discrepancies between theoretical simulation and experimental measurement are still remained.

Very recently, Beebe *et al.* have measured IET spectra for junctions formed from hexadecanethiol molecules with varying degrees of fluorination [14]. New insights into the vibronic coupling between the charge carriers and nuclear motions of the molecules, such as Raman modes are preferred over infrared modes, and an intensity of IETS related to a specific bond does not depend on the number of the bond have been concluded. This investigation not only explores the selection rules in IETS for a new series of molecules but also provides data for testing validity of theoretical models.

Basing on the early developed quantum chemical approach for electron transports in molecular junctions, Luo *et al.* developed a first-principles computational method with hybrid density functional theory [15, 16]. The vibronic coupling is introduced by expanding the electronic wave function over different vibrational normal modes within the harmonic approximation. This approach is successful to assign and interpret features of IETS given by experimental measurements [6, 7]. In order to understand the experimental observations given by Beebe *et al.* [14], we make a theoretical investigation on the molecular junctions formed by hexadecanethiol

molecular series.

2 Theoretical model

The molecular device is divided into three parts, source (S), drain (D), and extended molecule, as shown in Fig. 1. The source and drain are described by an effective mass approximation, while the extended molecule is treated with hybrid density functional theory at *ab initial* level. Our formality for the charge transport through molecular junction is based on Green's function theory, and it has been proven to have good descriptions for experimental measurements [6, 7, 15, 16]. For three-dimensional electrodes, the current density along molecular axis z is given as:

$$j_{SD} = \frac{4em^*k_{\mathrm{B}}T}{\hbar^3} \cdot \int_0^{\infty} \left\{ \ln \frac{1+\exp\left[(E_{\mathrm{F}}-E_z+eV_D)/k_{\mathrm{B}}T\right]}{1+\exp\left[(E_{\mathrm{F}}-E_z)/k_{\mathrm{B}}T\right]} \right\} \cdot |T(V_D,Q)|^2 n^S n^D \mathrm{d}E_z \quad (1)$$

where n^S and n^D are the density of states of the source and the drain, respectively, T is the device working temperature, m^* is the electron effective mass, and V_D is the external voltage. Here, E_{F} is the Fermi energy, which is taken as middle of highest occupied molecular orbital (HOMO) and lowest unoccupied molecular orbital (LUMO) of the extended molecule, and the nonequilibrium transport is considered by simple line-up the Fermi energy of the extended molecule and the bulk metals. The total current is $I = Aj_{SD}$, where A is the effective injection area of the transmitting electron. The transition matrix element from the source to the drain, $T(V_D, Q)$ is dependent on the vibrational motion Q and can be determined by

$$T(V_D,Q) = \sum_J \sum_K V_{JS}(Q) V_{DK}(Q) \sum_\mu g^\mu_{JK} \quad (2)$$

where $V_{JS}(Q)$ ($V_{DK}(Q)$) represents the coupling energy between the site $J(K)$ of the molecule and the reservoir $S(D)$ in the site representation; J and K run over the molecular sites; g^μ_{JK} is the carrier-conduction contribution from scattering channel ε_μ and can be written as:

$$g^\mu_{JK} = \left\{ \langle \Psi^\mu_0 + \sum_a \frac{\partial \Psi^\mu_0}{\partial Q_a} Q_a^{\nu\nu''} | K^\mu_0 + \sum_a \frac{\partial K^\mu_0}{\partial Q_a} Q_a^{\nu\nu''} \rangle \cdot \frac{\langle J^\mu_0 + \sum_a (\partial J^\mu_0/\partial Q_a) Q_a^{\nu'\nu} | \Psi^\mu_0 \rangle}{z_\mu - \varepsilon_\mu} \right\} + \left\{ \langle \Psi^\mu_0 + \sum_a \frac{\partial \Psi^\mu_0}{\partial Q_a} Q_a^{\nu\nu''} | K^\mu_0 + \sum_a \frac{\partial K^\mu_0}{\partial Q_a} Q_a^{\nu\nu''} \rangle \cdot \frac{\langle J^\mu_0 + \sum_a (\partial J^\mu_0/\partial Q_a) Q_a^{\nu'\nu} | \sum_a (\partial \Psi^\mu_0/\partial Q_a) Q_a^{\nu'\nu} \rangle}{z_\mu - \hbar\omega_a} \right\} \quad (3)$$

where $|J^\mu_0\rangle$ and $|K^\mu_0\rangle$ are the electronic function of the molecular site J and K at equilibrium position, respectively; and ω_a is the frequency for vibrational normal mode Q_a. Orbital $|\mu\rangle$ is the eigenstate of the Hamiltonian for the extended molecule. In the expression of g^μ_{JK}, the electronic wave function expanded as Taylor series along the vibrational normal mode is truncated to the first-order derivative with adopting the harmonic approximation, and the elastic off-resonant scattering regime is considered. Here, parameter z_μ is a complex variable, $z_\mu = E_\mu + \mathrm{i}\Gamma^{JK}_\mu$ with E_μ being the energy at which the scattering process is observed and Γ^{JK}_μ being the escape rate determined by the Fermi golden rule:

$$\Gamma^{JK}_\mu(Q) = \pi n^S V^2_{JS}(Q) \left|\langle J(Q) \mid \mu(Q)\rangle\right|^2 + \pi n^D V^2_{DK}(Q) \left|\langle \mu(Q) \mid K(Q)\rangle\right|^2 \quad (4)$$

From the current we can get the differential conductance as $\mathrm{d}I/\mathrm{d}V$. Taking the second derivative of the current, we get what we will refer to as the IET spectrum:

$$\frac{\mathrm{d}^2 I}{\mathrm{d}V^2} \quad (7)$$

which is often normalized with respect to the differential conductance, i.e.,

$$\frac{\mathrm{d}^2 I/\mathrm{d}V^2}{\mathrm{d}I/\mathrm{d}V} \quad (8)$$

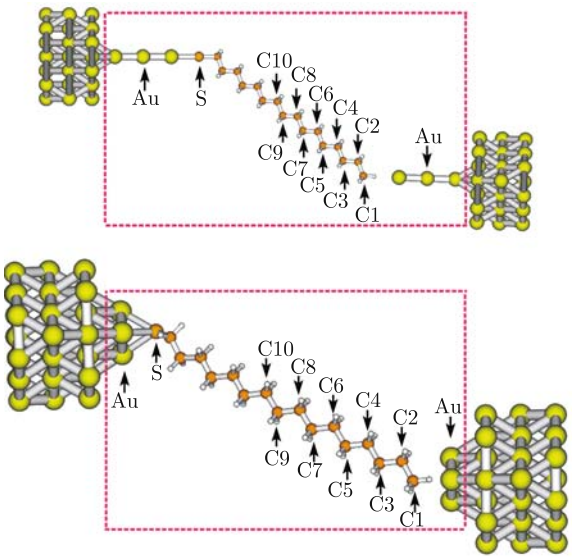

Fig. 1 Schematic structure of 1-hexadecanethiol molecular junction for a linear chain of three gold atoms and a triangle structure with three gold atoms. The fluorinated carbon atoms are noted.

3 Results and discussion

The semifluorinated alkanethiol junctions are noted as **F0**, **F1**, **F2**, **F3**, and **F10**, with the same nomenclature, as that in Ref. [14]. The IET spectra of the molecular junctions in three models are simulated. As a very simplified model to simulate the IETS, the first model ignores the influence of molecule–metal contact and takes the optimized structure of the gas-phase molecule, where the molecule–electrode coupling in the formalist is artificially introduced. This model is promised to clearly display the effect of the fluorine substitution in the molecules on IETS.

In the two other models, the influence of molecule-metal contact is considered. Here, contact atomic configurations of the linear chain and the triangle structure with three gold atoms are assumed (see Fig. 1). In the triangle configuration, the sulfur atom of the thiolate is located on the hollow position of three gold atoms with the S–Au bond length of 0.285 nm. We assume that the terminal hydrogen and fluorin atoms are at a given distance of 0.15 nm from the Au atom. The Au–Au bond length is fixed to be 0.288 nm for both cases. The molecular optimizations and frequency calculations have been performed at the B3LYP/Lanl2DZ level by using the Gaussian 03 program package [17]. The IETS is calculated using the QCME (Quantum Chemistry Molecular Electronics) program [18]. The temperature is taken as 4.2 K. A uniform broadening factor is set to be 4.0 meV for all simulated spectra.

The calculated IET spectra of semifluorinated alkanethiol series without considering the effect of metal-molecular contact are displayed in Fig. 2(a). In Fig. 2(a), one can see that these IET spectra are similar to each other. The assignments for the vibrational modes in our calculations have some resemblances with those in the calculated Raman spectra for each of the molecules. The C−F vibrational modes are not resolved in the IETS. With this simplified model, it seems to indicate that the Raman modes are preferred over infrared modes for contributing the scattering cross section. Five spectral peaks contributed from ν(C−S), CH_2 twisting, CH_2 wag, CH_2 scissoring, and CH_2 stretching modes are observed, and the strongest intensity is dominated by the CH_2 scissoring modes. Furthermore, by careful examination, we find that the peak at 1050 cm^{-1} is certainly due to the pure CH_2 twisting modes, and the ν(C−C) vibrational modes are absented in IETS, obtaining a different situation from that shown in Raman spectra.

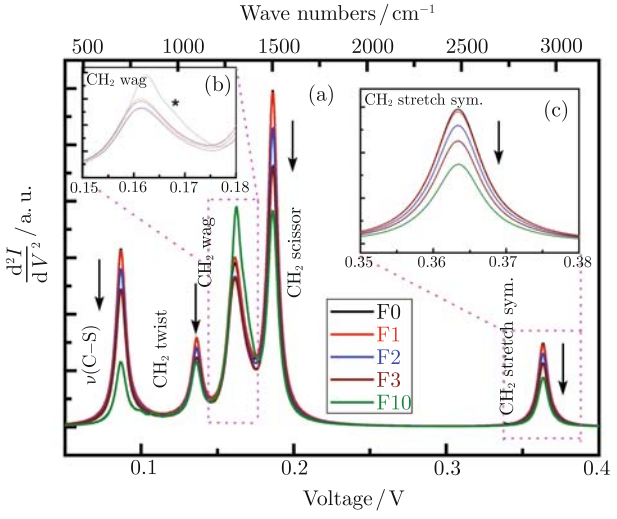

Fig. 2 **(a)** Illustration of the calculated IETS in gas phase for the semifluorinated hexadecanethiol series. The enlarged regions corresponding to CH_2 wagging and stretching modes are shown as insets in **(b)** and **(c)**, respectively.

It is interesting to note that there is a decrease in the peak intensities of ν (C−S) (720 cm^{-1}), CH_2 twisting (1120 cm^{-1}), CH_2 scissoring (1500 cm^{-1}), and CH_2 stretching modes (2950 cm^{-1}) when the number of fluorinated carbons increases from **F0** to **F10**. However, the variation of the intensity of the CH_2 wag modes at 1300 cm^{-1} is nonmonotonic for the number of fluorine atoms [see Fig. 2(b)], in which the intensity for molecule F10 takes the largest value. From these features, one at least can conclude that the IETS intensity is not a fully additive quantity.

For clarity, the region corresponding to the C−H stretching modes is enlarged, as shown in Fig. 2(c). It is observed that the IETS peaks of the vibrational modes for **F0** and **F1** take little difference. Note that the CH_3 group is replaced by the CF_3 group for molecule F1. The simulated results demonstrate that the C−H stretching modes contributed to peak at 2950 cm^{-1} are related to the CH_2 vibration and not to the CH_3 vibration. The further careful examination on the atomic vibration and frequency indicates that the peak is due to the symmetric stretching of the CH_2 group localized on the region directly adjacent to the sulfur atom. To our knowledge, the source of the C−H stretching mode was neither discussed nor correctly assigned. For instance, the theoretical calculations for alkanethiol molecules suggest that the peak of C−H stretching mode is related to the CH_3 vibration.

The calculated IET spectra of **F1** molecular junction for three situations considered, together with the corresponding experimental spectra are shown in Fig. 3. For the experimental spectrum of **F1** in Fig. 3(d), there exist four visible peaks, which are C−S stretching vibration at 94 mV, C−C stretching vibration at 135 mV, CH_2 wagging vibration at 173 mV, and CH_2 stretching vibration at 359 mV, respectively. In the triangle (gas-phase) case, the calculational ν(C−S) mode and CH_2 wagging and twisting mode (CH_2 wagging modes in gas-phase case) are found at 81.8(86.7) mV and 154.8(161.2) mV,

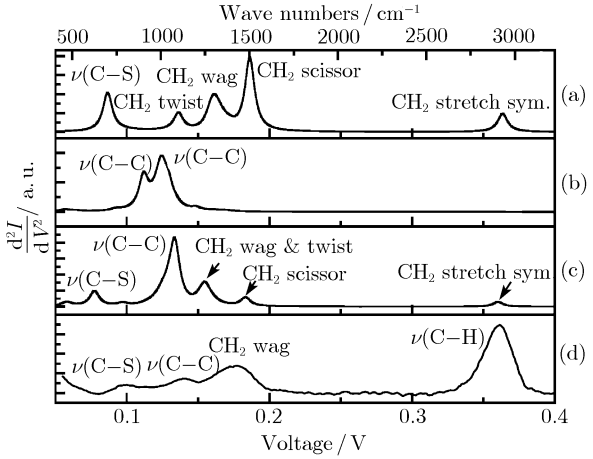

Fig. 3 ET spectra of **F1** for different cases: **(a)** The gas phase, **(b)** The chain contact, **(c)** The triangular contact, and **(d)** The experimental result.

respectively, which is in agreement with the experimental measurements of Wang *et al.* [4]. However, compared with the observed results of Beebe *et al.* [14], the ν(C−S) and CH_2 wagging and twisting modes are shifted down. Moreover, in the triangle and the gas-phase cases, the features at 183.2 mV and 186.2 mV respectively are due to the CH_2 scissoring vibrations. These vibrations come from the motions of CH_2 adjacent to the S atom and can also be assigned by other observed and calculated results [3, 4, 6−8]. Therefore, the experimental peak of CH_2 wagging vibration might be a sum of several spectral features, including not only the CH_2 wagging mode but also the CH_2 twisting and scissoring modes.

With the increase of the number of fluorinated carbons, the theoretical results for **F0**, **F2**, **F3**, and **F10** are also carried out for the linear chain case that are not shown in this paper. From these results, we find that the contributions of CH_2 stretching mode cannot be detected in the chain configuration for all semifluorinated alkanethiol molecules. Furthermore, comparing of the calculated IETS in the chain configurations with the experimental spectra, we notice that the calculated results do not fit with the experiments, which may imply that the contact structure for these molecular junctions should not be the chain configuration.

With the increase of the number of fluorinated carbons, the theoretical results in triangle cases for **F0**, **F1**, **F2**, **F3**, and **F10** are displayed in Fig. 4. Although there are C−F vibration modes in these semifluorinated alkanethiol series, the contribution of these modes to the IETS cannot be detected in our calculation, which is in agreement with the measured results. In Fig. 4, we can clearly see that the CH_2 stretching modes have contribution to IETS for all semifluorinated molecules, though the relative peak intensities of these modes are quite lower. Interestingly, it needs to note that there are contributions of C−C−C scissoring modes (belong to the fluorinated part of **F10**) to IETS. Since the calculated peaks of C−C−C scissoring modes are not found in other alkanethiol molecules, the contribution of these modes might be due to the fact that the number of the C−F bonds is more than that of C−H bonds in **F10**. Furthermore, the existence of C−C−C scissoring modes can partly explain the experimental red-shift of ν(C−C) mode in **F10**, namely, the experimental peak of ν(C−C) vibration should contain the contribution of C−C−C scissoring mode in the **F10** junction.

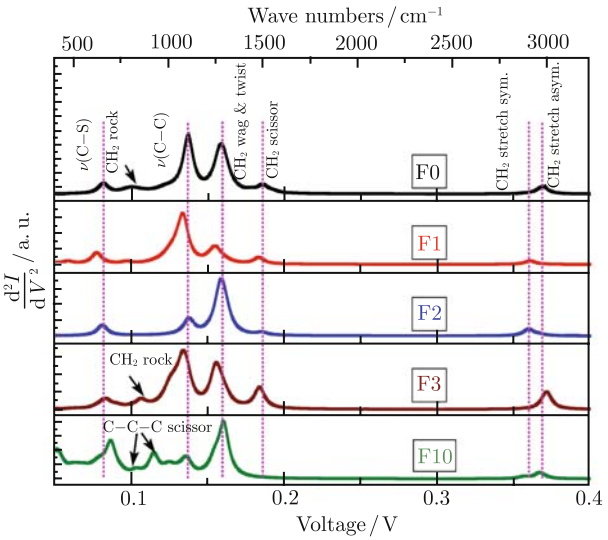

Fig. 4 Illustration of the calculated IETS for the semifluorinated hexadecanethiol series with triangular gold contacts.

We note that the contributions for the peak at around 155 mV are from CH_2 wagging and CH_2 twisting modes that often mix with each other in the "fingerprint region" [8]. In Fig. 4, it is interesting to note that there are frequency shifts of the vibrations depending on the odd or even numbers of the fluorinated carbon atoms in the region between 130 mV and 200 mV, while the similar shift can only be detected in the low energy region for **F10** in the experiment.

4 Conclusion

The IET spectra of semifluorinated hexadecanethiol series are investigated by using the Green's function-based scattering theory. We conclude that the linear Au trimer contact is not a possible contact for the semifluorinated molecular series. The theoretical IET spectra show the contribution of the CH_2 wagging, twisting, and scissoring modes, which corresponds to the "CH_2 wag" label in the experiment. The C−H stretching mode comes from the CH_2 vibration, which highly agrees with the experimental conclusion, and the stretching motion of the CH_2 group mainly comes from the one directly adjacent to the sulfur atom. Our results of semifluorinated alkanethiol series in the simple model support the conclusion

that the Raman modes are preferred over IR modes in IETS. Our calculations are helpful for understanding the experiment results presented by Beebe *et al.*.

Acknowledgements This work was supported by the National Natural Science Foundation of China (Grant No. 10674084) and the Natural Science Foundation of Shandong Province (Grant No. Z2007A02). The authors thank the support of the Swedish International Development Agency (SIDA) (348-2006-6679).

References

1. A. Troisi, M. A. Ratner, and A. Nitzan, J. Chem. Phys., 2003, 118(13): 6072
2. M. Galperin, M. A. Ratner, and A. Nitzan, J. Chem. Phys., 2004, 121(23): 11965
3. A. Pecchia, A. Di Carlo, A. Gagliardi, S. Sanna, T. Frauenheim, and R. Gutierrez, Nano Lett., 2004, 4(11): 2109
4. W. Wang, T. Lee, I. Kretzschmar, and M. A. Reed, Nano Lett., 2004, 4(4): 643
5. A. S. Hallbäck, N. Oncel, J. Huskens, H. J. W. Zandvliet, and B. Poelsema, Nano Lett., 2004, 4(12): 2393
6. J. Jiang, M. Kula, W. Lu, and Y. Luo, Nano Lett., 2005, 5(8): 1551
7. M. Kula, J. Jiang, and Y. Luo, Nano Lett., 2006, 6(8): 1693
8. G. C. Solomon, A. Gagliardi, A.Pecchia, T. Frauenheim, A. D. Carlo, J. R. Reimers, and N. S. Hush, J. Chem. Phys., 2006, 124(9): 094704
9. A. Troisi and M. A. Ratner, Phys. Chem. Chem. Phys., 2007, 9(19): 2421
10. D. P. Long, J. L. Lazorcik, B. A. Mantooth, M. H. Moore, M. A. Ratner, A. Troisi, Y. Yao, J. W. Ciszek, James M. Tour, and R. Shashidhar, Nature Mater., 2006, 5(11): 901
11. A. Troisi and M. A. Ratner, Nano Lett., 2006, 6(8): 1784
12. A. Troisi and M. A. Ratner, J. Chem. Phys., 2006, 125(21): 214709
13. J. R. Reimers, G. C. Solomon, A. Gagliardi, A. Bili, N. S. Hush, T. Frauenheim, A. Di Carlo, and A. Pecchia, J. Phys. Chem. A, 2007, 111(26): 5692
14. J. M. Beebe, H. J. Moore, T. R. Lee, and J. G. Kushmerick, Nano Lett., 2007, 7(5): 1364
15. C. K. Wang, Y. Fu, and Y. Luo, Phys. Chem. Chem. Phys., 2001, 3: 5017
16. J. Jiang, M. Kula, and Y. Luo, J. Chem. Phys., 2006, 124(3): 034708
17. M. J. Frisch, G. W. Trucks, et al., Gaussian 03, Gaussian, Inc., Pittsburgh PA, 2003
18. Jun Jiang, Chuan-kui Wang, and Yi Luo, Quantum Chemistry for Molecular Electronics (QCME-V1.1), Sweden: Royal Institute of Technology, 2006